# AUTOMATIC DETECTION OF OPTIC DISC BASED ON PCA AND STOCHASTIC WATERSHED

*Sandra Morales*[1*], *Valery Naranjo*[1], *David Pérez*[1], *Amparo Navea*[2], *Mariano Alcañiz*[1,3]

[1] Instituto Interuniversitario de Investigación en Bioingeniería y Tecnología Orientada al Ser Humano, Universitat Politècnica de València, I3BH/LabHuman, Camino de Vera s/n, 46022 Valencia, Spain
[2] Fundación Oftalmológica del Mediterráneo, Valencia, Spain
[3] Ciber, Fisiopatología de Obesidad y Nutrición, CB06/03 Instituto de Salud Carlos III, Spain

## ABSTRACT

The algorithm proposed in this paper allows to segment the optic disc from a fundus image. The goal is to facilitate the early detection of certain pathologies and to fully automate the process so as to avoid specialist intervention. The method used for the extraction of the optic disc contour is based on a variant of the watershed transformation, the stochastic watershed. A principal component analysis (PCA) and a previous pre-processing, focused on mathematical morphology, are performed in order to prepare the image for segmentation. The purpose of using PCA is to obtain the grey-scale image that better represents the original RGB image. The implemented algorithm has been validated on a public database obtaining promising results.

***Index Terms—*** Optic disc, optic nerve head, stochastic watershed, principal component analysis

## 1. INTRODUCTION

Optic disc (OD) detection is a key process in many algorithms designed for the automatic extraction of anatomical ocular structures and the detection of retinal lesions. Its automatic location would provide useful information to determine regions of interest in a fundus image, as well as for the early detection of certain pathologies. For example, it is directly related to diseases such as glaucoma and knowing its location would also help to reduce the number of false positives in the detection of exudates associated with diabetic retinopathy.

In general, the techniques presented in the literature about the OD processing from fundus images can be grouped into two categories: location and segmentation methods. Location methods are based on finding the OD center and segmentation algorithms on estimating its contour. Location methods are usually focused on the fact that all retinal vessels originate from the OD and follow a parabolic path [1, 2] or that the OD is the brightest component on the fundus [3, 4]. Among segmentation methods, several approaches must be stressed: templated-based algorithms [5, 6], deformable models [7, 8] and morphological techniques [9, 10]. Most of algorithms based on mathematical morphology detect the OD by means of watershed transformation, generally through marker-controlled watershed, although each author proposes the use of different markers.

The method presented in this paper incorporates some of the aforementioned techniques besides new contributions. It is mainly based on watershed transformation with markers, in the same way that in [9, 10], although with certain improvements: First, a principal component analysis (PCA) is applied on the RGB fundus image obtaining a grey image in which the different structures of the retina, such as vessels and OD, are differentiated more clearly in order to get a more accurate detection of the OD. This stage is very important since it largely determines the final result. Then, the vessels are removed through morphological operations to make the segmentation task easier. Finally, the required markers are randomly selected, instead of using controlled markers, and a variant of the watershed transformation, the stochastic watershed transformation, is implemented. This algorithm is fully automatic, so the process is sped up and user intervention is avoided making it completely transparent.

The paper is organized as follows: in Section 2 the main stages of the proposed method are described, including the principal component analysis, the morphological operations performed as well as the stochastic watershed transformation. Section 3 shows the experimental results and the validation obtained using a public database. Finally, Section 4 provides conclusions, discussion and some future work lines.

## 2. METHOD

In this paper, an automatic method to detect the optic disc is presented. It is focused on using stochastic watershed trans-

*E-mail address: smorales@labhuman.i3bh.es. This work has been funded by the project IMIDTA/2010/47 and partially by projects Consolider-C (SEJ2006-14301/PSIC), "CIBER of Physiopathology of Obesity and Nutrition, an initiative of ISCIII" and Excellence Research Program PROMETEO (Generalitat Valenciana. Conselleria de Educación, 2008-157).

 

formation on a fundus image to obtain the optic disc contour. Previously, a pre-processing of the original RGB image is required. The first step of the pre-processing consists of applying PCA to transform the input image to grey scale. This technique combines the most significant information of the three components RGB in a single image so that it is a more appropriate input to the segmentation method.

### 2.1. PCA algorithm

Generally, an initial grey image is necessary to carry out most of the segmentation algorithms of the literature. However, in the case of the OD segmentation, each author considers appropriate a different intensity image, from a band of the original RGB image [6, 9] to a component of the other colour space [7]. In this work, the use of a new grey-scale image is proposed. Specifically, it is calculated by means of PCA [11]. This type of analysis maximizes the separation of the different objects that compose the image so that the structures of the retina are better appreciated. In addition, it is much less sensitive to the existing variability in a fundus image regarding colour, intensity, etc.

For a RGB image $\mathbf{f}(\mathbf{x}) = (f_R(\mathbf{x}), f_G(\mathbf{x}), f_B(\mathbf{x}))$, the result of the PCA algorithm is a new image defined as

$$g = \boldsymbol{\alpha}'\mathbf{f} = \alpha_R f_R + \alpha_G f_G + \alpha_B f_B \qquad (1)$$

where $\alpha_R$, $\alpha_G$ and $\alpha_B$ are each element of the eigenvector associated with the largest eigenvalue of the covariance matrix

$$\boldsymbol{\Sigma} = \begin{pmatrix} \sigma_R^2 & \sigma_{RG} & \sigma_{RB} \\ \sigma_{RG} & \sigma_G^2 & \sigma_{GB} \\ \sigma_{RB} & \sigma_{GB} & \sigma_B^2 \end{pmatrix}, \qquad (2)$$

being the elements of this matrix the empiric covariance of the RGB components of $\mathbf{f}$.

This new image $g$ must contain the most structural contrast and information of the three original channels. Therefore, it must be proved that the largest eigenvalue represents a 90% of the total sum of eigenvalues.

Fig. 1(a) shows an original fundus image and Fig. 1(b) its grey-scale image obtained by PCA. Note that the whole image is processed although only a region of interest is shown for better visualisation.

### 2.2. Mathematical morphology

Mathematical morphology [12] is a non-linear image processing methodology based on minimum and maximum operations whose aim is to extract relevant structures of an image.

By applying a morphological closing on the grey-scale image obtained by the PCA algorithm, the blood vessels that are within the OD are removed, which facilitates its detection, as seen in Fig. 1(c). A circular structuring element is used in that operation whose radius must be bigger than the radius of the largest vessel, for example in a 600x400 image the chosen

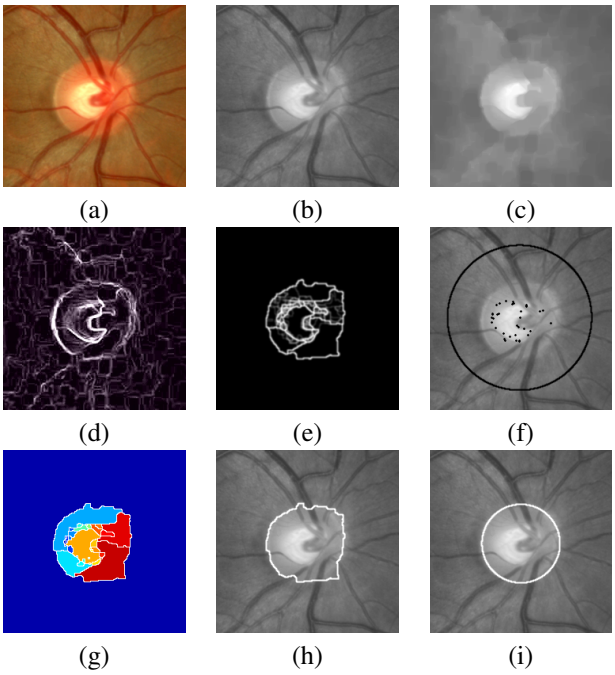


**Fig. 1**. Different stages of the proposed method: (a) Original image, (b) Gray-scale image obtained by PCA, (c) Morphological closing, (d) Gradient image, (e) Probability density function of contours using 5 simulations and 50 internal markers, (f) Internal and external markers, (g) Stochastic watershed regions, (h) Stochastic watershed contour and (i) Circular approximation.

radius was 7. After that, applying a threshold is easier. This threshold is calculated based on a percentage of the brightest pixels of the image. Specifically, the region will be formed by the lightest zone of the image whose area is a 3% of the total area of the image (this is the average percentage usually occupied by the OD on a fundus image). The result of this thresholding is a binary image whose largest object will be a part of the OD. Then, a series of markers are generated using this object, which will be useful when the watershed transformation is applied in order to regenerate the complete contour of the OD.

### 2.3. Stochastic watershed transformation

The watershed transformation [12] is a segmentation technique for grey-scale images. This algorithm is a powerful segmentation method whenever the minima of the image represent the objects of interest and the maxima are the separation boundaries between objects. Due to this fact, the input image of this method is usually a gradient image (Fig. 1(d)). In mathematical morphology, the gradient $\varrho(f)(\mathbf{x})$ of an image $f(\mathbf{x})$ is obtained as the pointwise difference between a unitary dilation and a unitary erosion, i.e.,

$$\varrho(f)(\mathbf{x}) = \delta_B(f)(\mathbf{x}) - \varepsilon_B(f)(\mathbf{x}). \quad (3)$$

However, one problem of this technique is the over-segmentation, which is caused by the existence of numerous local minima in the image normally due to the presence of noise. One solution to this problem is using markers, which artificially indicate the minima of the image. Although the controversial issue consists in determining the markers for each region of interest. Note that the use of few markers along with the existence of borders within the OD can also cause that some parts of it are not detected (sub-segmentation). Therefore, the choice of the correct markers is crucial for the effectiveness and robustness of the algorithm.

A watershed transformation variant is used to solve this conflict, the stochastic watershed [13]. In this transformation, a given number $M$ of marker-controlled-watershed realizations are performed selecting $N$ random markers in order to estimate a probability density function ($pdf$) of image contours and filter out non significant fluctuations (Fig. 1(e)). Let $\{f_{mrki}\}_{i=1}^{M}$ be $M$ sets of $N$ random markers and $WS_i = WS(\varrho)_{f_{mrki}}$ the $i$th output image of the marker-controlled watershed imposed by $f_{mrki}$. The $pdf$ of image contours is computed by Parzen window method [14] as follows

$$pdf(\mathbf{x}) = \frac{1}{M}\sum_{i=1}^{M}(WS_i(\mathbf{x}) * G(\mathbf{x}; s)) \quad (4)$$

where $G(\mathbf{x}; s)$ represents a Gaussian kernel of variance $\sigma^2$ and mean $\mu$ ($\mu = 0$)

$$G(\mathbf{x}; s) = \frac{1}{2\pi\sigma^2} e^{-\left(\frac{\|\mathbf{x}\|^2}{2\sigma^2}\right)}. \quad (5)$$

Despite using random markers, a restriction on the randomness of these markers is imposed to avoid segmenting unwanted regions of the fundus. First, a number $N$ of uniform random markers are generated within of the thresholded region mentioned above. Secondly, the number of valid markers is limited to those which are situated in pixels whose intensity is similar to the intensity of an initial seed belonging to the object to be segmented. It is due to the fact that some of them can not be located in an appropriate place because this region can contain pixels out of the OD. So that, only the markers situated in the most intense pixels, which ensures that they are located within the OD, are taking into account. In our case, the chosen seed $\mathbf{x_0}$ is the geodesic center of the largest object selected. More precisely, the algorithm to generate an image, $f_{out}(\mathbf{x})$, which contains non-uniform pseudo-random markers from an initial image, $f(\mathbf{x})$, is as follows:

1. Initialize the output image: $f_{out}(\mathbf{x}) = 0$.
2. Consider that $f(\mathbf{x})$ follows a Gaussian distribution: $F(\mathbf{x}) = e^{-\left(\frac{f(\mathbf{x})-f(\mathbf{x}_0)}{\sigma'}\right)^2}$, where $\sigma'^2$ is equal to the variance of the largest object region multiplied by a tolerance value obtained experimentally, i.e., $\sigma'^2 = t \cdot \sigma^2$ with $t = 10$.
3. Compute cumulative distribution function: $cdf(\mathbf{x}_i) = \frac{\sum_{k\leq i} F(\mathbf{x}_k)}{\sum_{k=1}^{P} F(\mathbf{x}_k)}$, being $P$ the number of pixels of $f(\mathbf{x})$.
4. Generate $N$ uniform random markers, $\mathbf{r} = (r_1, ..., r_N)$.
5. for $j = 1$ to $N$
6. Find the smallest value $s_j$ such that $r_j \leq cdf(\mathbf{x}_{s_j})$.
7. $f_{out}(\mathbf{x}_{s_j}) = 1$.

On the other hand, in the marker definition not only internal markers (that specify what is the object of interest) are needed, but also an external marker which limits the area to be segmented. The internal markers will be pseudo-random markers generated as explained up above, and the chosen external marker will be a circle centred on the geodesic center of the largest object whose radius is equal to two times the radius of this area. See Fig. 1(f).

Obtaining a $pdf$ of the contours of the watershed regions facilitates the final segmentation, providing robustness and reliability since the arbitrariness in choosing the markers is avoided. Afterwards, the $pdf$ can be combined with the initial gradient in order to reinforce the gradient contours which have a high probability resulting a probabilistic gradient [13],

$$\rho(\mathbf{x}) = (1 - \lambda)\varrho(f)(\mathbf{x}) + \lambda pdf(\mathbf{x}) \quad (6)$$

with $\lambda = 0.5$ the results are in general satisfactory.

Finally, a last marker-controlled watershed is applied to $\rho(\mathbf{x})$ using a new set of non-uniform pseudo-random markers. The final OD-segmentation is obtained as the union of all watershed regions of this transformation.

### 2.4. Circular approximation

Once the region of interest has been obtained by the watershed transformation, the result must be adjusted to eliminate false contours, which are detected due generally to the blood vessels that pass through the OD. The morphological closing was initially performed to remove them, as previously mentioned, although it is not enough because some irregularities can still be appreciated in the watershed contour (Fig. 1(h)).

In the literature, a final OD approximation is usually done through ellipses or circles. In our work, we have adjusted the OD by a circle because this algorithm will later be used to establish a zone of the retina concentric to the OD to perform retinal vessel diameter measurements according to a standard protocol [15]. The fit is performed by means of Kasa's method [16] which lets calculate the center and the radius of the circle that better is adapted to a binary region through least squares. Fig. 1(g) shows the different regions obtained by the

stochastic watershed transformation, Fig. 1(h) its contour and Fig. 1(i) its circular approximation.

## 3. RESULTS

The validation of the method has been carried out on the public database DRIONS [17]. In DRIONS database 110 fundus images are included with their OD manually segmented by two different specialists. Because of the OD selected by the specialists lacked of circular shape, the same circular approximation applied to our results has also been performed on the manual segmentations. The first observer images have been taken as reference (gold standard) to calculate similarity degree between them and our segmentation. Moreover, the segmented images by the second observer have also been compared with the gold standard to obtain inter-expert differences.

The performance of the method has been evaluated based on five concepts. Jaccard's (JC) and Dice's (S) coefficients describe similarity degree between two compared elements being equal to 1 when segmentation is perfect. Accuracy (Ac) is determined by the sum of correctly classified pixels as OD and non-OD divided by the total number of pixels in the image. True positive fraction (TPF) is established by dividing the correctly classified pixels as OD by the total number of OD pixels in the gold standard. Finally, false positive fraction (FPF) is calculated by dividing the misclassified pixels as OD by the total number of non-OD pixels in the gold standard. In Table 1 these results can be observed. In summary, the average values obtained are: JC=0.7783, S=0.8579, Ac=0.9901, TPF=0.8064, FPF=0.0021. In this table our results can be compared with the $2^{nd}$ observer results as well as the results obtained by the implementation of other existing technique based on marker-controlled-watershed transformation [9].

**Table 1**. Comparison between the results of the proposed method, $2^{nd}$ observer and other marker-controlled-watershed algorithm (average values and standard deviations) regarding the gold standard.

| | **Proposed method** | **$2^{nd}$ observer** | **Walter et al. [9]** |
|---|---|---|---|
| **JC** | 0.8120 (0.2055) | 0.8876 (0.0349) | 0.5990 (0.3506) |
| **S** | 0.8774 (0.1718) | 0.9401 (0.0207) | 0.6683 (0.3756) |
| **Ac** | 0.9921 (0.0100) | 0.9948 (0.0016) | 0.9659 (0.0507) |
| **TPF** | 0.8689 (0.1955) | 0.9316 (0.0452) | 0.6602 (0.3874) |
| **FPF** | 0.0034 (0.0062) | 0.0023 (0.0010) | 0.0226 (0.0423) |

## 4. CONCLUSION AND DISCUSSION

From a fundus image, the implemented algorithm is able to automatically locate the OD. This method tries to make easier the early detection of diseases related to the fundus. Moreover, it has been validated on a public database obtaining promising results.

The main advantage is the full automation of the algorithm. It does not require any intervention by clinicians, which releases necessary resources (specialists) and reduces the consultation time. For those reasons, its use in primary care is facilitated.

Variability between fundus images in colour, intensity, size, presence of artefacts, etc. makes each state-of-the-art method uses a different input image: the green [6] and red [9, 10] band of the original RGB image, a combination of both of them [5], or the intensity component extracted from the HSI representation [7], among others. However, due to this fundus image variability, they do not always provided the desired results, therefore a PCA, able to maximize the separation between the different objects of the image, has been proposed in this paper as input image more appropriate. PCA has already been used as a starting point for segmentation, tracking or detection in image processing [18, 19]. In Fig. 2, PCA is compared with the use of the red component on a specific image. It can be observed that while the red component is completely over-saturated, PCA obtains a grey image where the OD could be segmented.

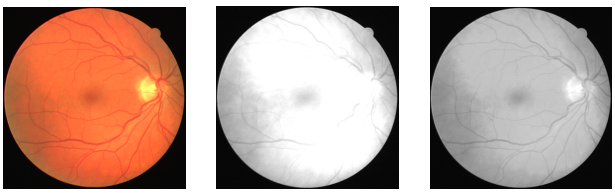

(a) (b) (c)

**Fig. 2**. Advantadges of PCA: (a) Original RGB fundus image, (b) Red component and (c) Image obtained by PCA.

On the other hand, improvements achieved by the stochastic variant in relation to other marker-controlled watershed must also be highlighted. The use of several simulations with random markers helps to avoid sub-segmentation problems, as occurs in Fig. 3 where the original image, shown in Fig. 1(a), has been segmented as [9] using only one internal marker located in the geodesic center of its largest and brightest object.

Due to the complexity of the fundus images, their high number of elements makes a perfect segmentation difficult. That is the reason for which a circular approximation is applied on the segmented disc.

As for future lines, the optic cup will also be detected. Its goal will be to measure the cup-to-disc (C/D) ratio so that it can be used for glaucoma diagnosis. A high C/D ratio will indicate that a fundus is suspicious of glaucoma.

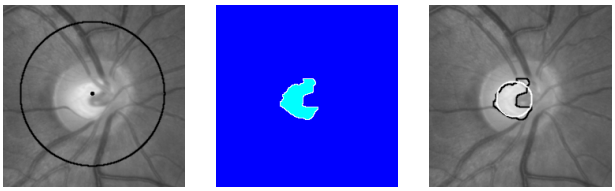

(a) (b) (c)

**Fig. 3**. Sub-segmentation problem produced in other marker-controlled-watershed method: (a) Internal and external marker, (b) Marker-controlled-watershed region, and (c) Contour of watershed region in black and its circular approximation in white.

## 5. REFERENCES


[1] A. Hoover and M. Goldbaum, "Locating the optic nerve in a retinal image using the fuzzy convergence of the blood vessels," *Medical Imaging, IEEE Transactions on*, vol. 22, no. 8, pp. 951 –958, 2003.

[2] M. Foracchia, E. Grisan, and A. Ruggeri, "Detection of optic disc in retinal images by means of a geometrical model of vessel structure," *Medical Imaging, IEEE Transactions on*, vol. 23, no. 10, pp. 1189 –1195, 2004.

[3] S. Chaudhuri, S. Chatterjee, N. Katz, M. Nelson, and M. Goldbaum, "Automatic detection of the optic nerve in retinal images," in *IEEE International Conference on Image Processing*, 1989, vol. 1, pp. 1–5.

[4] S. C. Lee, Y. Wang, and E. T. Lee, "Computer algorithm for automated detection and quantification of microaneurysms and hemorrhages (HMAs) in color retinal images," in *SPIE Conference on Image Perception and Performance*, 1999, vol. 3663, pp. 61–71.

[5] A. Aquino, M.E. Gegúndez-Arias, and D. Marín, "Detecting the optic disc boundary in digital fundus images using morphological, edge detection, and feature extraction techniques," *Medical Imaging, IEEE Transactions on*, vol. 29, no. 11, pp. 1860 –1869, 2010.

[6] M. Lalonde, M. Beaulieu, and L. Gagnon, "Fast and robust optic disc detection using pyramidal decomposition and hausdorff-based template matching," *Medical Imaging, IEEE Transactions on*, vol. 20, no. 11, pp. 1193 –1200, 2001.

[7] J. Lowell, A. Hunter, D. Steel, A. Basu, R. Ryder, E. Fletcher, and L. Kennedy, "Optic nerve head segmentation.," *IEEE Trans. Med. Imaging*, vol. 23, no. 2, pp. 256–264, 2004.

[8] J. Xu, O. Chutatape, E. Sung, C. Zheng, and P. Chew Tec Kuan, "Optic disk feature extraction via modified deformable model technique for glaucoma analysis," *Pattern Recognition*, vol. 40, pp. 2063–2076, 2007.

[9] T. Walter, J. C. Klein, P. Massin, and A. Erginay, "A contribution of image processing to the diagnosis of diabetic retinopathy-detection of exudates in color fundus images of the human retina," *Medical Imaging, IEEE Transactions on*, vol. 21, no. 10, pp. 1236–1243, 2002.

[10] D. Welfer, J. Scharcanski, C. M. Kitamura, M. M. Dal Pizzol, L. W. B. Ludwig, and D. R. Marinho, "Segmentation of the optic disk in color eye fundus images using an adaptive morphological approach," *Computers in Biology and Medicine*, vol. 40, no. 2, pp. 124 – 137, 2010.

[11] J. C. Russ, *Image Processing Handbook*, CRC Press, Inc., 5th edition, 2007.

[12] P. Soille, *Morphological Image Analysis: Principles and Applications*, Springer-Verlag New York, Inc., 2nd edition, 2003.

[13] J. Angulo and D. Jeulin, "Stochastic watershed segmentation," in *Proc. of the 8th International Symposium on Mathematical Morphology*, 2007, pp. 265–279.

[14] R. O. Duda and P. E. Hart, *Pattern Classification and Scene Analysis*, John Wiley & Sons Inc, 1973.

[15] T. Y. Wong, M. D. Knudtson, R. Klein, B. E. K. Klein, S. M. Meuer, and L. D. Hubbard, "Computer-assisted measurement of retinal vessel diameters in the beaver dam eye study: methodology, correlation between eyes, and effect of refractive errors.," *Ophthalmology*, vol. 111, no. 6, pp. 1183–1190, 2004.

[16] C. A. Corral and C. S. Lindquist, "On implementing kasa's circle fit procedure," *IEEE Transactions on Instrumentation and Measurement*, vol. 47, no. 3, pp. 789–795, 1998.

[17] E. J. Carmona, M. Rincón, J. García-Feijoó, and J. M. Martínez-de-la-Casa, "Identification of the optic nerve head with genetic algorithms," *Artif. Intell. Med.*, vol. 43, pp. 243–259, 2008.

[18] M. Goffredo, M. Schmid, S. Conforto, M. Carli, A. Neri, and T. D'Alessio, "Coarse-to-fine markerless gait analysis based on PCA and Gauss-Laguerre decomposition," in *Proc. SPIE Medical Imaging*, 2005, vol. 5747, pp. 1076–1084.

[19] Avraham Levy and Michael Lindenbaum, "Sequential karhunen-loeve basis extraction and its application to images.," *IEEE Transactions on Image Processing*, vol. 9, no. 8, pp. 1371–1374, 2000.